Faceted interfacial structure of $\{10\bar{1}1\}$ twin in Ti formed during equal channel angular pressing

Y.J. Li[a)], Y.J. Chen [b)], J.C. Walmsley [a)], R. H. Mathinsen [c)], S. Dumoulin [a)] and H. J. Roven [b)]

[a] SINTEF Materials and Chemistry, 7465, Trondheim, Norway
[b] Department of Materials Science and Engineering, NTNU, 7491, Trondheim Norway.
[c] Department of Physics, NTNU, 7491, Trondheim, Norway.

Abstract

The boundary structure of $\{10\bar{1}1\}$ deformation twins formed in commercial pure titanium (CP-Ti) during the initial pass ECAP processing has been studied by TEM and HRTEM. A new twining mode with twinning dislocation of $b_{3/3}$, has been identified by a dichromatic diagram method. The new mode of $\{10\bar{1}1\}$ twin has substantially higher interface energy and accommodates more shear strain during deformation than the conventional b_4 twinning mode. The deviation angle between the habit trace of the twin boundary and the theoretical twinning plane, K1, is dependent upon the density of twin dislocations.

Over the last decades, severe plastic deformation (SPD) has been demonstrated as an effective method to produce bulk ultra-fine grained (UFG) and nano structured metals, for example Al, Mg, Fe, Ni and Ti, as reviewed in [1,2]. Much work has been done on the deformation behaviour of face centred cubic (FCC) metals during SPD [3-5]. However, studies on the deformation behaviour, especially the twinning behaviour of hexagonal close packed (HCP) structures, like Ti, have been limited.

Shin et al.[6, 7] studied the deformation behaviour of a commercial pure titanium (CP-Ti) during the initial passes of equal channel angular pressing (ECAP) at $350^{o}C$. It was found that the shear strain (~1.8) imposed during the 1st pass of ECAP is mainly accommodated by $\{10\bar{1}1\}$ deformation twins. Since the normal twinning structure , of $\{10\bar{1}1\}$ twins, the so called b_4 mode, for which the subscript is the step height of the twinning dislocations on the twin boundary in number of the theoretical twin planes, can only accommodate a shear strain of ~0.1 [8,9], the authors suggested that the $\{10\bar{1}1\}$ twins formed during ECAP might have different twinning modes, which can accommodate a much higher shear strain than b_4 mode.

Pond and Serra et al. have done a series of atomic scale computer simulations on the twinning structures of HCP metals [10-12]. The simulation results show that $\{10\bar{1}1\}$ twins can have different interfacial structures, including a dislocation-free single atom plane twin boundary structure and faceted twinning boundaries with b_2, b_3 and b_4 twinning dislocations. Among the simulated twinning structures, only the fully relaxed dislocation-free single atom plane twin boundary[13] and the b_2, b_4 mode twinning[10,14] have been observed in Ti by HRTEM.

In a recent work by Kim et al. [15], the authors claimed that they found b_1, b_2 and b_3

modes of $\{10\bar{1}1\}$ twin formed during the initial pass ECAP processing in a HRTEM

study. However, the quality of the HRTEM images of the twin boundary structures in

the work is poor and the identification of the twin dislocations is ambiguous. The

aim of the present work is to shed more light upon the interfacial structures of

$\{10\bar{1}1\}$ twins formed in CP-Ti during SPD.

As-rolled and annealed CP-Ti rods with dimensions of 20 mm x 20mm x120mm were

pressed in a 90° ECAP die at $450\,^oC$ with a pressing speed of 2 mm/s. After pressing

the samples were quenched into cold water. Specimens for transmission electron

microscopy (TEM) were taken from the central longitudinal section of the middle part

of the ECAP bar and prepared by mechanical polishing followed by twin jet electro

polishing with a solution of 5% perchloric acid, 35% butanol, and 60% methanol. The

electro polishing was conducted at -40 ^oC and 40V. Microstructure studies of the

ECAPed samples were conducted in a JEOL 2010F TEM equipped with a field

emission gun (FEG) operating at 200 kV. This microscope has a point- resolution of

0.23 nm.

TEM studies show that a large fraction of parallel narrow twin bands have formed

during the 1st pass ECAP. The width of most of the bands is in the range of 100- 300

nm. The typical morphology of the twin bands is shown in Fig. 1a. Selected area

electron diffraction (SAED) patterns taken on the twin bands, show that they are

formed by $\{10\bar{1}1\}$ deformation twinning. Fig. 1b shows a SAED taken on two of the

neighbouring bands in Fig.1a, along the $[1\bar{2}10]$ zone axis. The trace of the theoretical

twinning plane $(10\bar{1}1)$ is also drawn in Fig. 1a. Clearly, the habit trace of the twin boundary, especially at the tip of the twin band, deviates from the theoretical twin plane.

A HRTEM image of the twin boundary close to the twin tip, marked with the rectangular box in Fig. 1a, is shown in Fig. 1c. As can be seen, the twinning boundary shows a faceted structure.

In order to get a clearer image of the atomic structure in the above twin boundary, Fourier filtration has been applied to produce filtered HRTEM images of the twin boundary. As shown in Fig. 2, the twin boundary is consisting of a series of steps (marked with bright lines) joining straight terraces (marked with dark lines). The terraces are parallel to the $(10\bar{1}1)$ planes, while the steps are closely parallel to the prism planes of the matrix, $(10\bar{1}0)_m$, and the $(10\bar{1}3)$ planes of the twin crystal. The heights of the steps on the boundary have been counted to be 2d(K1), 3d(K1) and 4d(K1), where, d(K1) is the spacing of the $(10\bar{1}1)$ twinning planes. It is interesting to find that the height of the same step at the twin side can be different from that at the matrix side. According to the heights of the steps, the twinning dislocations around the steps are denoted as $b_{p/q}$, where p and q are the number of K1 planes in height in the matrix side and the twin crystal side, respectively. Therefore, the defects around the three steps in Fig. 2, from the upper left to the lower right side, are denoted as $b_{3/3}$, $b_{2/3}$ and $b_{3/4}$ respectively. HRTEM images have been taken at several locations of the twin tip. It shows that most of the step defects in the twin boundary investigated belong to one of these three types of dislocations. In addition to the dislocations in the

twin boundary, stacking faults (SF) can also be observed frequently in the twin crystals, as marked in Fig. 2.

The dichromatic diagram method developed by Pond et al. [16] was applied to draw Burgers circuits around individual steps in the boundary. The Burgers vectors of the twinning dislocations are calculated by applying the topological theory of Pond [17]. The same approach has been applied in many other studies [10-12,18,19]. The calculated Burgers vectors of the twinning dislocations are shown in Table 1. For comparison, the simulated b_2 and b_4 mode twinning dislocations of $\{10\bar{1}1\}$ twins by Serra et al. [12] are also included in the table.

The $b_{3/3}$ twinning dislocation has a rational Burgers vector, $[\,\bar{1}01\bar{2}\,]$, which is consistent with the simulated b_3 twinning dislocation [10, 11], confirming experimentally the simulated twinning mode. The $b_{2/3}$ and $b_{3/4}$ dislocations have irrational Burgers vectors and have never been simulated or observed in the $\{10\bar{1}1\}$ twin boundary of Ti. They are probably formed by the reaction between slip dislocations and the twin boundary. The $b_{2/3}$ dislocation is proposed to be formed by the reaction of $\,$ <c> type slip dislocations with a Burgers vector of [0001] with the twin boundary: <c> $\rightarrow$ $b_{2/3}$ + $b_{3/3}$. As a result, the <c> dislocation dissociates into a twining dislocation $b_{3/3}$ and a step defect $b_{2/3}$. However, how the $b_{3/4}$ defect is formed is yet to be understood.

It should be noted that a similar faceted interfacial boundary structure of $\{10\bar{1}1\}$ twins in a Zr-2.5wt% Nb alloy formed during heat treatment has been reported by

Weatherly et al. [19], where the step planes, however, are found to be parallel to the set of {0002} and {$10\bar{1}\bar{1}$} planes of the twin crystals.

The shear strain of the twinning boundaries can be calculated by $s = |b|/h$, where $|b|$ is the magnitude of Bugers vectors and h is the height of steps, for $b_{2/3}$, $h = 2d(K1)$ and for $b_{3/4}$, $h = 3d(K1)$. As can be seen from Tab. 1, the shear strains of $b_{2/3}$ and $b_{3/4}$ dislocations are very close to $b_{3/3}$ dislocation, which are much higher than that of the b_4 twinning dislocation. Since the elastic energy of the dislocations is proportional to the square of the Burgers vector, the elastic energy of the twin boundary formed during ECAP is also much higher than that of the twinning boundary formed by b_2 and b_4 modes, implying that high shear strain and high energy twin boundaries have formed during the SPD process.

It has been shown in Fig.2 that the twin boundary trace deviates strongly from the theoretical twinning planes. In practice, the {$10\bar{1}1$} twin boundary habit planes in different HCP materials are often observed to deviate from the theoretical twinning planes. For example, the habit plane of {$10\bar{1}1$} twinning boundaries formed during heat treatment in Zn-2.5%wtNb is closely parallel to the ($30\bar{3}5$) planes [19]; the habit of {$10\bar{1}1$} deformation twins in Mg is close to the ($30\bar{3}4$) planes [20]. Though not discussed, the habit of the {$10\bar{1}1$} twins formed during ECAP of CP-Ti in reference [6] also deviates from the theoretical twinning planes. The deviation in Mg was found to be due to double twinning of {$10\bar{1}1$} + {$10\bar{1}2$} twin [21, 22]. However, no double twinning has been found in ECAPed Ti and Zr-2.5wt%Nb. The deviations in the two

materials can easily be ascribed to the step-terrace structure of the twin boundaries, where the steps change the trace of the twin boundary planes.

Fig. 3 shows a schematic diagram of the step-terrace structure in the $\{10\bar{1}1\}$ twin boundary. The deviation angle, θ, can be calculated by the step heights and terrace length using the equation, $\tan\theta = h/(h\cdot\gamma+L)$, where, γ is the axial ratio of HCP crystals (for Ti, γ =1.586) and L is the length of a terrace between two neighbouring steps. The deviation angle increases with the step height and the density of steps. Accordingly, the same relation can be used also to estimate the density of twinning dislocations, if the step heights and deviation angle are known. Although it is difficult to find the real tip of $\{10\bar{1}1\}$ twins in ECAP Ti, the twin boundaries at one end of the twin bands (Fig. 1a), which have much higher deviation angles from $\{10\bar{1}1\}$ planes than in the interior of the bands, are believed to be close to the twin tips. This implies that the densities of twinning dislocations or stress concentration at the boundary of twin tips are higher than in the boundaries behind tips. This has been confirmed by HRTEM observations (not shown here) that the average terrace length is much larger in the boundary far behind twin tips. The low dislocation density in the twin boundary far behind the twin tip is presumably due to the stress relaxation.

Although the twinning shear of the $\{10\bar{1}1\}$ twins observed in the present work has been found to be as high as about 0.5, it can only accommodate a part of the total strain subjected during the first pass ECAP. The grain boundary structure of the 1 pass ECAP-Ti in the present work has been studied by electron back-scattered diffraction (EBSD) [23]. It shows that twinning has only occurred on less than half of

the grains in the material, implying that a large part of the deformation strain has to be accommodated by dislocation slip. As strong evidence of the important roll of dislocation slip, a large fraction of low angle grain boundaries (LAGB) and a large amount of equiaxed ultrafine grains are seen to have formed in CP-Ti after one ECAP pass. This is different from the results of Shin et al., where, twinning occurred in most of the grains [6]. This difference may be ascribed to the deformation temperature used in the present work, 450 ^{o}C, which is substantially higher than in the work of Shin et al.

As a summary, the interfacial structure of the $\{10\bar{1}1\}$ twinning boundary formed in CP-Ti during the 1st pass ECAP has been observed by HRTEM. The step defects in the twin boundary have been identified by a dichromatic method. The $\{10\bar{1}1\}$ twin has been found to be formed by the $b_{3/3}$ twinning mode. The twinning boundary shows a high energy, high shear strain and faceted step-terrace structure. The step-terrace twinning interfacial structure is suggested to be responsible for the deviation of the habit twinning boundary planes from the theoretical ones. The deviation angle can be calculated by the step height and terrace length.

Reference

[1] R. Z. Valiev and T. G. Langdon, Prog. Mater. Sci. 51(2006) 881.
[2] R.Z. Valiev, R.K. Islamgaliev, I.V. Alexandrov, Prog. Mater. Sci, 45(2000) 103.
[3] J.Y. Huang, Y.T. Zhu, H. Jiang, and T.C. Lowe, Acta Mater. 49 (2001).1497
[4] Z. Horita, D.J. Smith, M. Nemoto, R.Z. Valiev, T.G. Langdon. J. Mater. Res. 13(1998) 446
[5]. R.Z. Valiev, C. Song, S.X. McFadden, A.K. Mukherjee, R.S. Mishra, Philos. Mag. A 81 (2001)25
[6] D.H. Shin, W.J. Kim and W.Y. Choo, Scripta mater. 41, 259(1999).
[7] D. H. Shin, I. Kim, J. Kum, Y. S. Kim and S. L. Semiatin, Acta mater. 51, 983 (2003).
[8] N.E. Paton and W.A. Backofen, Trans. TMS-AIME, 245(1969) 1369.
[9] N. E. Paton and W. A. Bacofen, Metall. Trans. 1(1970)2839

[10] R.C. Pond, D.J. Bacon and A. Serra, Phil. Mag. Lett. 71(1995) 275.
[11] A. Serra, R.C. Pond and D.J. Bacon, Acta metall. Mater.39(1991) 1469
[12] A. Serra, D.J. Bacon and R.C. Pond, Acta metall. 36(1988) 3183
[13] Y.C. Wang, D.H. Ping, D.X. Li and H.Q. Ye, Phil. Mag. Lett. 74(1996) 367
[14] Y. Kasukabe, Y. Yamada, P.J. Lin and L.A. Burill, Phil. Mag. Lett. 67(1993) 361
[15] I. Kim, J. Kim, D.H. Shin, X.Z. Liao, Y.T. Zhu, Scripta Mater. 48(2003) 813.
[16] R.C. Pond and J. P. Hirth, Solid St. Phys. 47(1994) 288
[17] R. C. Pond, Dislocations in Solids, vol. 8 (Amsterdam: North Holland, 1989), edited by F. R. N. Nabarro, p. 1.
[18] T. Braisaz, P. Ruterana, G. Nouet and R.C. Pond, Phil.Mag. A. 75(1997) 1075
[19] G. C. Weatherly, A. Perovic and V. Perovic, Phil. Mag. A. 79(1999) 2071
[20] R. E. Reed-Hill and W. D. Robertson, Acta Met. 5(1957) 717
[21] S. L. Couling, J. F. Pashak, and L. Sturkey, Trans. Met. Soc. AIME, 224(1963)70
[22] J.W Christian, S. Mahajan, Progr. Mater. Sci. 39 (1995)1.
[23] Y. J. Chen, Y.J. Li, , J. C. Walmsley and H. J. Roven, to be published.

Captions of table and figures

Table 1 Parameters of dislocations on $\{10\bar{1}1\}$ twin boundary, $K_1 = (10\bar{1}1)$, $\Lambda = \left(\frac{3}{2}\right)^{1/2} \frac{c}{a}$

Fig. 1 Morphology of $\{10\bar{1}1\}$ twinning bands (a), selected electron diffraction pattern of a twinning boundary along $[1\bar{2}10]$ zone axis (b), and HRTEM image of the twinning boundary boxed in (a) along $[1\bar{2}10]$ zone axis (c).

Fig. 2 Inverse fast Fourier transform (IFFT) image of the Fourier filtered image in the boxed area shown in Fig. 1c. Burgers circuits are drawn around three step defects. In the figure, the steps are parallel to $(10\bar{1}0)_m$, and $(10\bar{1}3)_t$, and the terraces are parallel to $\{10\bar{1}1\}$.

Fig. 3 Schematic diagram showing the deviation angle between the twin boundary trace and the twin plane caused by the step-terrace structure of the faceted twinning boundary.

Table 1 Parameters of twin dislocations on $\{10\bar{1}1\}$ twin boundary, $K_1=(10\bar{1}1)$, $\Lambda = \left(\tfrac{3}{2}\right)^{1/2}\tfrac{c}{a}$

Dislocation	Burgers vector	$h/d(K_1)$	$\lvert b\rvert$, nm	Strain, **s**
b₂	$\frac{1}{(6\Lambda^2+3)}\left[5-2\Lambda^2,-2\Lambda^2-1,4\Lambda^2-4,6\Lambda^2-9\right]$	2	0.176	0.393
b₄	$\frac{(2\Lambda^2-3)}{(2\Lambda^2+1)}\left[\bar{1}012\right]$	4	0.086	0.096
b₂/₃	$\frac{1}{(2\Lambda^2+1)}\left[2\Lambda^2-2,0,2-2\Lambda^2,5-2\Lambda^2\right]$	2	0.238	0.530
b₃/₄	$\frac{1}{2(2\Lambda^2+1)}\left[6\Lambda^2-5,0,5-6\Lambda^2,12-8\Lambda^2\right]$	3	0.306	0.455
b₃/₃	$\frac{(2\Lambda^2-2)}{(2\Lambda^2+1)}\left[\bar{1}012\right]$	3	0.331	0.492

Note: parameters for b₂ and b₄ dislocations are from reference [11].
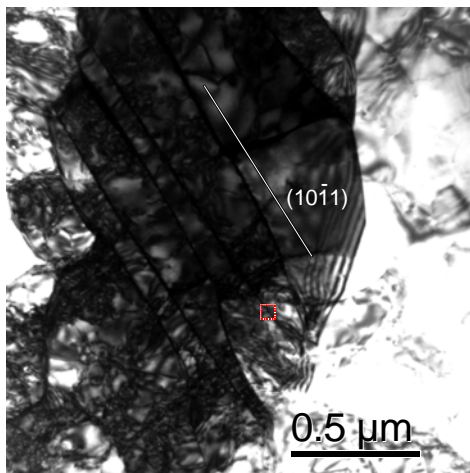
(a)
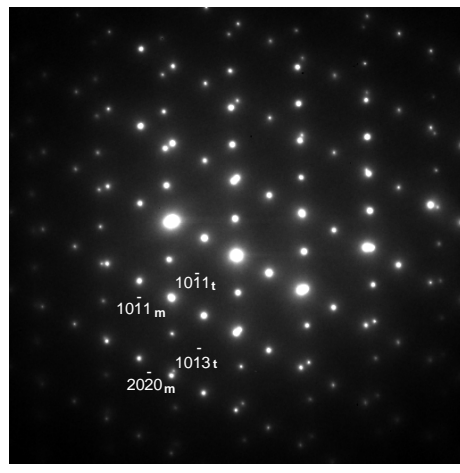
(b)
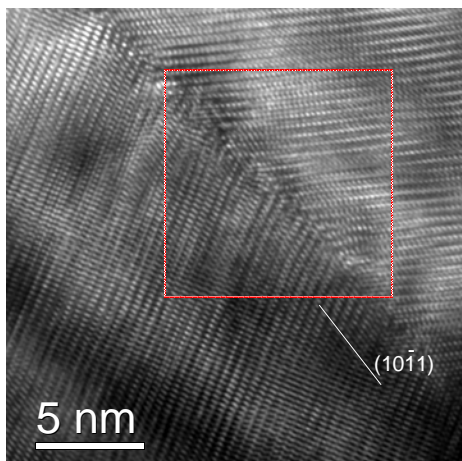
(c)

Fig. 1 Morphology of $\{10\bar{1}1\}$ twinning bands (a), selected electron diffraction pattern of a twinning boundary along $[1\,\bar{2}\,10]$ zone axis (b), and HRTEM image of the twinning boundary boxed in (a) along $[1\,\bar{2}\,10]$ zone axis (c).
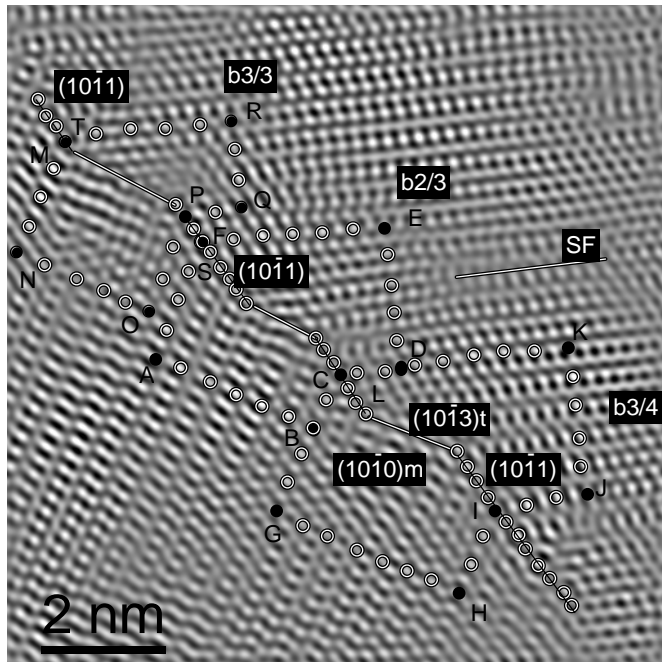
Fig. 2 Inverse fast Fourier transform (IFFT) image of the boxed area shown in Fig. 1c. Burgers circuits are drawn around three steps. . In the figure, the steps are parallel to $(10\bar{1}0)_m$, and $(10\bar{1}3)_t$, and the terraces are parallel to $\{10\bar{1}1\}$.


Fig. 3 Schematic diagram showing the deviation angle between the twin boundary trace and the twin plane caused by the step-terrace structure of the faceted twinning boundary.